

Crustal conductivity footprint of the orogenic gold district in the Red Lake greenstone belt, western Superior craton, Canada

Ademola Q. Adetunji¹, Gaetan Launay¹, Ian J. Ferguson², Jack M. Simmons¹, Chong Ma¹, John Ayer¹ and Bruno Lafrance¹

¹Mineral Exploration Research Centre (MERC), Harquail School of Earth Sciences, Laurentian University, Sudbury, ON P3E2C6, Canada

²Department of Earth Sciences, University of Manitoba, Winnipeg, MB R3T2N2, Canada

ABSTRACT

A magnetotelluric (MT) study across the Red Lake greenstone belt of the western Superior craton, Canada, images a 50-km-long north-dipping conductor (<20 Ω·m) at 20–25 km depth and subvertical conductors spatially correlated with crustal-scale shear zones and large orogenic gold deposits. The conductors are interpreted to be the conductivity signature of the deep crustal source of the auriferous fluids and pathways of the orogenic gold system. The geophysical results, supported by existing geochemical and fluid inclusion studies, suggest that the Au- and CO₂-rich fluids responsible for gold mineralization were released by devolatilization of supracrustal rocks underthrust to mid- to lower-crustal levels during subduction. This MT study links shallow gold mineralization to a deep crustal source region, demonstrating the connection between a crustal suture zone and the formation of orogenic gold deposits in an Archean greenstone belt.

INTRODUCTION

The Uchi terrane of the Superior craton (Canada) comprises Meso-Neoproterozoic metavolcanic, metasedimentary, and plutonic rocks. It hosts multiple orogenic gold deposits extending along the southern margin of the North Caribou terrane (Sanborn-Barrie et al., 2001). The Red Lake greenstone belt (Fig. 1) deposits are among the largest and the richest Archean gold deposits in Canada (Dubé et al., 2004; Chi et al., 2006) and have produced >839,000 kg Au (Lewis et al., 2021). The formation of such orogenic gold deposits requires a confluence of first-order factors, including a thermal source, a deep hydrothermal fluid system, and commonly an oblique-slip regime late in the orogenic cycle of a convergent margin (e.g., Goldfarb and Groves, 2015; Groves et al., 2020). Current interpretations of the Red Lake greenstone belt gold deposits are consistent with this model (e.g., Dubé et al., 2004; Chi et al., 2009, 2022). Multiple studies have shown that the magnetotelluric (MT) method can image crustal-scale fluid pathways and the fluid source regions associated with world-class mineralization (e.g., Heinson et al., 2018, 2021; Hill et al., 2021; Vadoodi et al., 2021; Comeau et al., 2022; Kirkby et al., 2022). Here, we use MT imaging to delineate crustal-scale electrical conductors below the Red Lake greenstone belt

in order to constrain the source and pathways of the Au-bearing fluids and to contribute to the understanding of auriferous mineral systems in Archean greenstone belts.

TECTONIC AND GEOLOGICAL SETTING

The Uchi terrane and adjacent margin of the North Caribou terrane record 300 m.y. of tectonic events starting with rifting at ca 2.99 Ga and followed by protracted continental arc magmatism at 2.94–2.91, 2.90–2.89, 2.85, and 2.75–2.72 Ga (Sanborn-Barrie et al., 2001; Percival et al., 2006a, 2006b), including formation of the 2.745–2.695 Ga Berens River plutonic complex in the North Caribou terrane (Corfu and Stone, 1998; Percival et al., 2006b).

Convergence between the North Caribou terrane and terranes from the south culminated in subduction-driven thrusting of the Winnipeg River terrane crustal block under the North Caribou terrane during the Kenoran orogeny at 2.72–2.70 Ga (Sanborn-Barrie et al., 2001). Evidence for an active subduction system includes the intrusion of the Berens River felsic plutonic suite (Corfu and Stone, 1998). Metasedimentary rocks in the English River terrane, which separate the Winnipeg River and Uchi terranes (Fig. 1), are interpreted as backarc or foreland basin deposits (Corfu et al., 1995; Sanborn-

Barrie et al., 2004). Geometry of crustal-scale seismic reflections indicative of crustal thinning beneath the Winnipeg River and English River terranes and localized deposition of late orogenic alluvial-fluvial sedimentary rocks are interpreted to reflect a period of crustal extension that occurred after the amalgamation of the Winnipeg River terrane with the Uchi–North Caribou terranes at ca. 2.698 Ga (e.g., Calvert et al., 2004; Hrabí and Cruden, 2006; Percival, 2007).

Deformation in the Red Lake greenstone belt produced the main penetrative structures during a protracted D₂ event related to collision of the Winnipeg River and North Caribou terranes between ca. 2.723–2.712 Ga. It involved reactivation of earlier D₁ fabrics and greenschist-facies metamorphism (Gallagher et al., 2018) and was followed by emplacement of post-tectonic plutons and cooling by 2.70 Ga (Corfu et al., 1995; Percival et al., 2006b). Post-collisional D₃ strain occurred after 2.70 Ga, overprinting and reactivating earlier structures (e.g., Sanborn-Barrie et al., 2004) synchronous with peak, amphibolite-facies metamorphism associated with the post-orogenic intrusions (Gallagher et al., 2018). Shear zones of varying scale formed during both the D₂ and D₃ deformation events (Percival, 2007).

The main-stage Red Lake greenstone belt mineralization, associated with D₂, occurred before 2.712 Ga and includes the largest and highest-grade deposits in the Red Lake “mine trend” (RLMT in Fig. 1; Dubé et al., 2004; Sanborn-Barrie et al., 2004). Fluid inclusion and isotope studies indicate that H₂O-poor, CO₂-dominated fluids, potentially derived from granulite-facies metamorphism in deeper parts of the crust, were responsible for the carbonate veining and mineralization (Chi et al., 2006, 2009). Late-stage Au mineralization occurs as very high-grade mineralization in 2.702–2.701 Ga lamprophyre dikes and may have been associated with D₃ strain and metamorphism (Dubé et al., 2004).

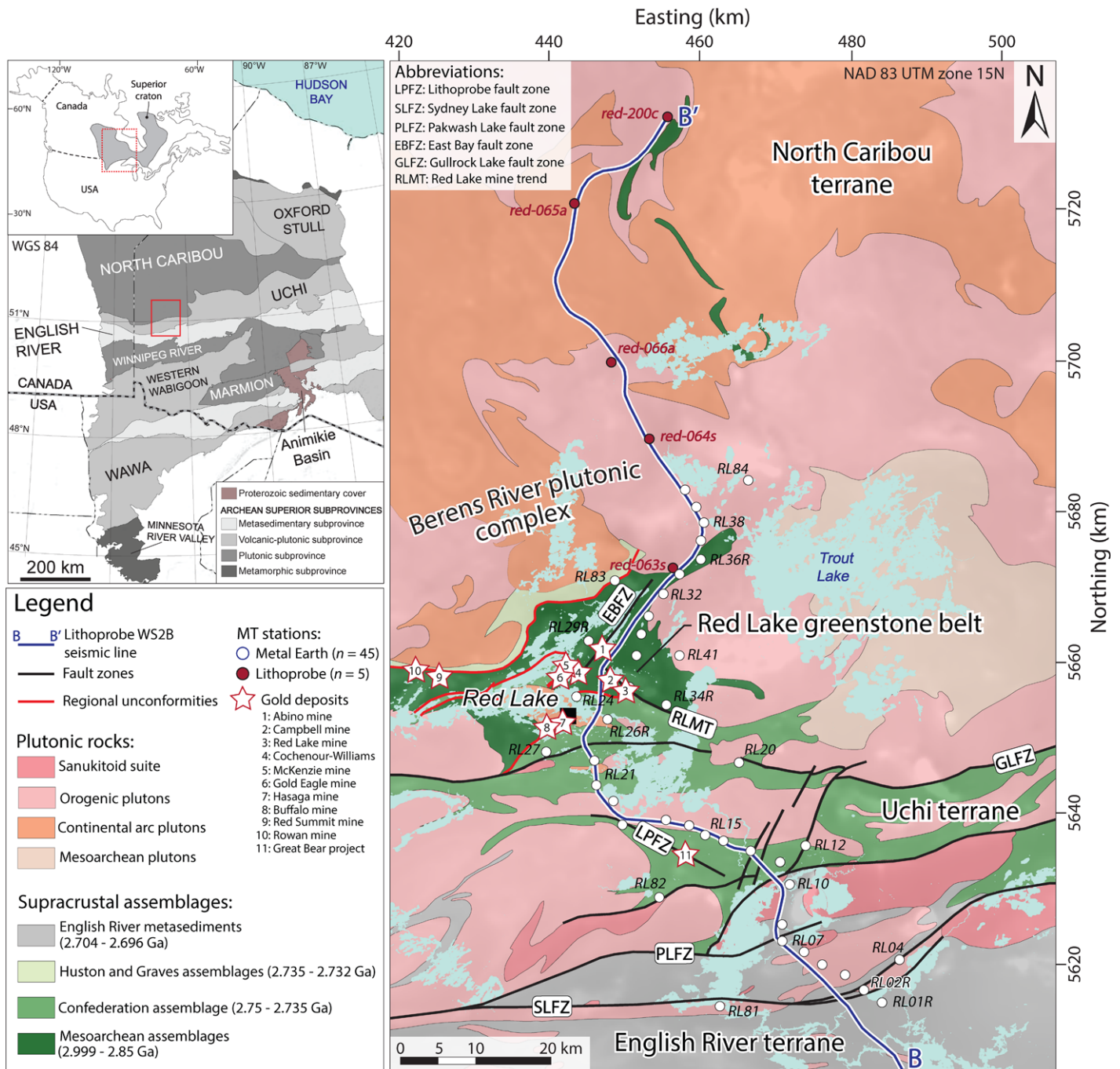


Figure 1. Geological map of study area, western Superior craton, Canada (modified from Sanborn-Barrie et al., 2004), showing magnetotelluric (MT) locations (red and white circles), Lithoprobe WS2B seismic reflection profile (blue line), and Au mineralization (white stars). Coordinate system abbreviations: WGS 84—World Geodetic System 1984; NAD 83—North American Datum of 1983; UTM—Universal Transverse Mercator.

METHOD AND RESULTS

Forty-five (45) broadband MT sites were occupied by Quantec Geoscience Limited (Toronto, Canada) in 2020, along a transect that aligns with seismic profile WS2B of the Lithoprobe project (Calvert et al., 2004). Additional MT sites located off the main profile provide some three-dimensional (3-D) control (Fig. 1). The profile was extended to the northern end of the seismic line using five broadband MT sites from the Lithoprobe Western Superior transect. Evaluation of the MT data set using the MT

phase tensor method indicates phase-skew magnitudes of predominately $>3^\circ$, confirming the existence of large-scale 3-D structures in the region (see the Supplemental Material¹).

Resistivity models were created using the ModEM 3-D inversion algorithm (see the Sup-

plemental Material). Input data consisted of the six components of the MT transfer functions for 50 sites with error floors of 5% on all impedance components and of 0.03 on tipper. The preferred model converged to a normalized root-mean-square misfit of 1.96. Representative slices of the resistivity model are shown in Figure 2. Major resolved structures, whose existence and geometry have been confirmed with model hypothesis testing, are labeled R1–R2 and C0–C4 for resistive and conductive features, respectively.

¹Supplemental Material. Details of MT imaging and resolution tests and supplemental figures. Please visit <https://doi.org/10.1130/GEOL.S.21936003> to access the supplemental material, and contact editing@geosociety.org with any questions.

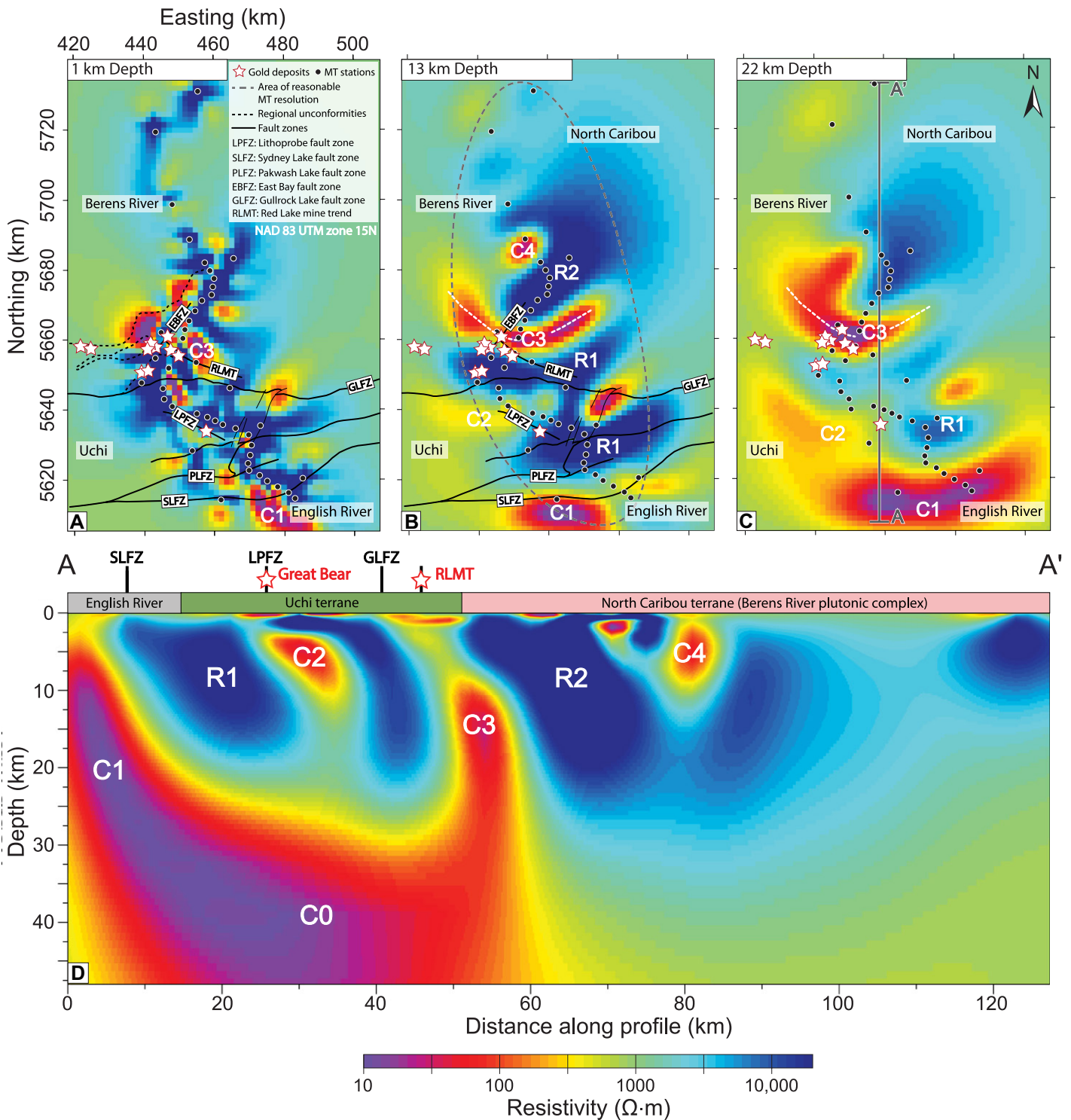


Figure 2. (A–C) Resistivity model showing horizontal slices at upper-crustal (A), mid-crustal (B), and lower-crustal (C) depths. MT—magnetotelluric. (D) Cross section extracted from the three-dimensional model along the line A–A' indicated in panel C. Black dots show the MT locations and white stars show Au deposits. R1–R2 and C0–C4 are resistive and conductive features, respectively. Coordinate system abbreviations: NAD 83—North American Datum of 1983; UTM—Universal Transverse Mercator.

The resistivity model defines a generally resistive 2000–10,000 $\Omega \cdot m$ upper crust (R1 and R2 in Fig. 2). The lower crust of the North Caribou terrane is less resistive (<1000 $\Omega \cdot m$). To the south, there is a laterally extensive north-dipping conductor C0 (<20 $\Omega \cdot m$), with its top at 20–25 km depth. Conductors C1, C2, and C3 are

large-scale subvertical conductivity anomalies. The uppermost crust (<5 km depth) beneath the Red Lake mine trend is relatively resistive, with the resistivity of some parts >20,000 $\Omega \cdot m$. In contrast, the shallow crust in the Berens River plutonic complex contains several localized conductors (C4).

INTERPRETATION

The well-resolved conductors beneath the study area are interpreted to represent the conductivity signature of altered rocks and structures associated with the orogenic gold system in the Red Lake greenstone belt formed during the last major tectonic events between the North

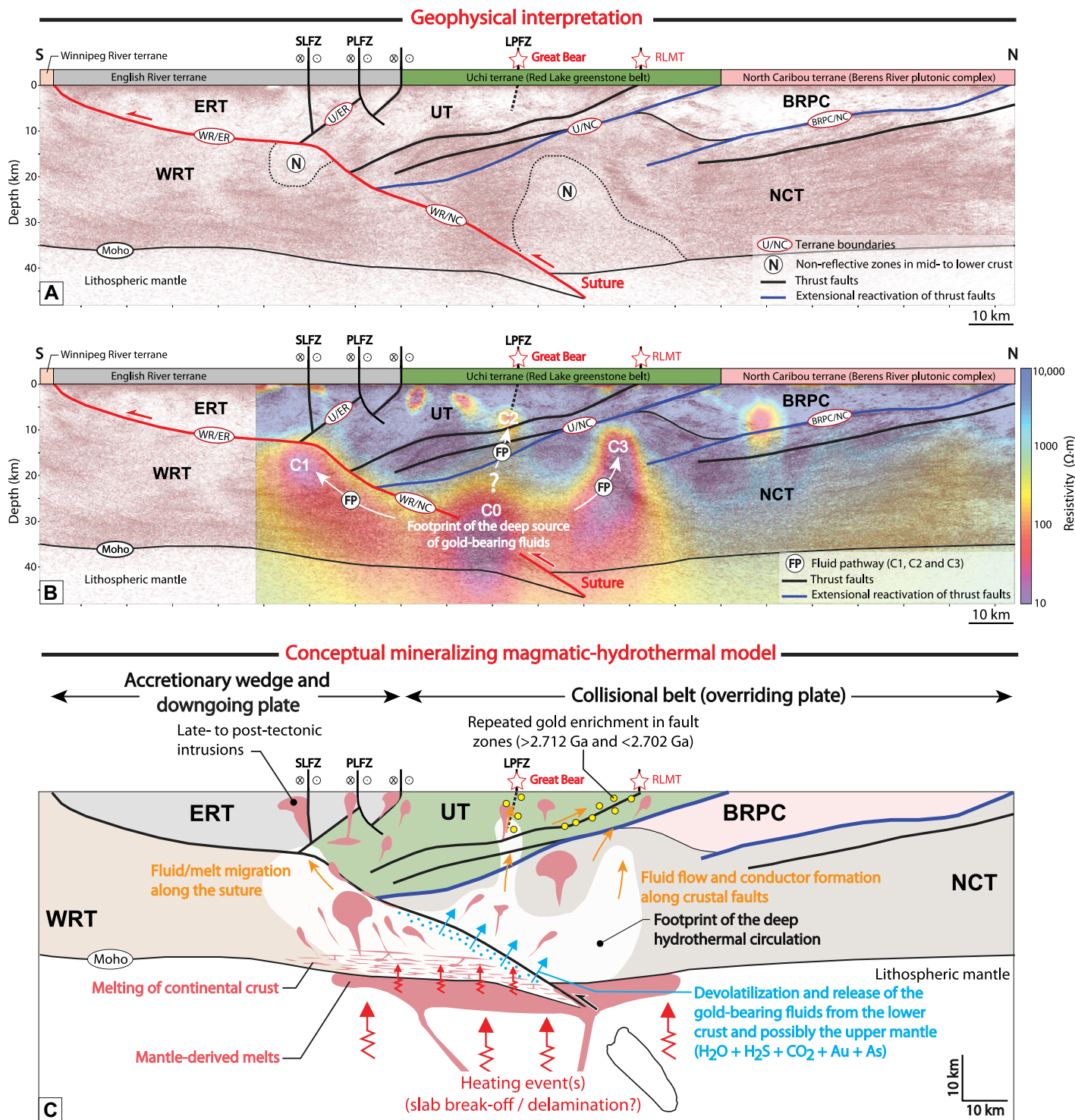


Figure 3. (A) Lithoprobe seismic reflection data for line WS2B from Calvert et al. (2004) showing features interpreted in current study. See Calvert et al. (2004) and van der Velden (2007) for detailed and alternative interpretations of the data. (B) Overlay of seismic reflection line WS2B with coincident (crooked-line) vertical resistivity section along WS2B. Note slightly different geometry of resistivity results from those in line A-A' in Figure 2. (C) Illustration of interpreted conceptual mineral system model showing tectonic features, heat source, and fluid pathways to upper-crustal depths. C0–C3 are conductive features. SLFZ—Sydney Lake fault zone; PLFZ—Pakwash Lake fault zone; LPFZ—Lithoprobe fault zone; RLMT—Red Lake mine trend; ERT—English River terrane; WRT—Winnipeg River terrane; UT—Uchi terrane; BRPC—Berens River plutonic complex; NCT—North Caribou terrane; FP—Fluid pathway.

Caribou and Winnipeg River terranes (Dubé et al., 2004; Fig. 3).

Crustal-scale conductor C1 coincides with significant north-dipping seismic reflections that extend into the mantle interpreted to rep-

resent the suture associated with subduction of the Winnipeg River terrane beneath the North Caribou terrane (Calvert et al., 2004; van der Velden, 2007). Seismic reflection results from Lithoprobe line WS1, located 250 km to the east,

also provide evidence for northward subduction (White et al., 2003; Percival et al., 2006b). MT studies around the world have imaged conductors at crustal and mantle depths associated with subducting plates, with anomalies attributed to

fluids produced by devolatilization of the subducted sediments and/or interaction of these fluids with surrounding rocks (e.g., Wannamaker et al., 2009; Ye et al., 2019). The geometry of C1 is consistent with subduction-related devolatilization and transport of fluids along the subducting plate. The interpretation of subducted metasediments beneath the Red Lake greenstone belt is inferred from the implied subduction, seismic and electromagnetic results, and the geochemistry of plutonic rocks (e.g., Corfu and Stone, 1998). Sedimentary sequences within the dominantly granitic gneisses of the Winnipeg River terrane are documented southeast of the study area (e.g., Sanborn-Barrie and Skulski, 2006).

Inversion hypothesis tests require conductor C0 to be located at middle- to lower-crustal depths (see the Supplemental Material). There is evidence that C0 formed as a result of metamorphic devolatilization of subducted supracrustal rocks. Firstly, in the vicinity of C0, the seismic reflection data include short north-dipping reflectors parallel to the suture in a zone that van der Velden (2007) interpreted as a subduction complex. Farther east, line WS1 includes an accretionary imbricate stack at a similar depth (White et al., 2003). Secondly, geochemical and fluid inclusion studies of Au mineralization at Red Lake suggest mineralizing fluids were derived from granulite facies metamorphism in deeper parts of the crust (Chi et al., 2006, 2009). Subducted marine sediments could also provide a source to explain the high $\delta^{13}\text{C}$ ratios in fluid inclusions in the Red Lake deposits (Gallagher et al., 2018). Thirdly, geochemistry of Berens River tonalite and granite suites suggests the melts interacted with partial melting of greywacke at low pressure and low H_2O content (Corfu and Stone, 1998). MT studies elsewhere provide evidence for metasedimentary rocks forming source regions of Au-bearing fluids. Heinson et al. (2021) interpreted a $<20 \Omega\cdot\text{m}$ resistivity zone at >20 km depth beneath the Lachlan orogenic gold field in southeastern Australia as the source region for gold-rich fluids resulting from reactions in carbon- and pyrite-rich sedimentary rocks under amphibolite conditions at $\sim 550^\circ\text{C}$, leading to both the production of Au-rich fluids and the formation of flake graphite at grain boundaries in permeable zones.

Additional support for C0 being related to devolatilization of subducted supracrustal rocks stems from conductors C2 and C3 representing possible fluid pathways beneath major Au deposits in the Red Lake greenstone belt. Previous imaging of fluid pathways beneath other ore deposits (Heinson et al., 2018; Vadoodi et al., 2021; Comeau et al., 2022) supports this interpretation. C3 lies directly below the Red Lake mine trend with its top at 10 km and extending to depths >15 km, is consistently imaged as a

subvertical feature, and most likely connects with C0 (see the Supplemental Material). C3 also lies in a region of reduced reflectivity, as has been observed for other deposit-forming fluid pathways (Heinson et al., 2018). Both resistivity and seismic results at depths >10 – 15 km are thus consistent with fluid transport along a steep fault system. There are complex seismic reflection responses in the upper crust above C3. In the upper 10 km beneath the Red Lake mine trend, shear zones have moderate dips to the south (Fig. 3) with varying interpretations (Calvert et al., 2004; Zeng and Calvert, 2006; van der Velden, 2007). Geobarometry of the Berens River plutonic complex indicates 6–7 km of uplift relative to surrounding areas, leading van der Velden (2007) to suggest that the low seismic reflectivity may also be the result of steeply dipping structures accommodating the uplift.

The location of C2 is fairly well resolved (see the Supplemental Material) and coincides with the Great Bear deposit located adjacent to the Lithoprobe fault (Fig. 3; Zeng and Calvert, 2006; Lewis et al., 2021). The geometry of C2 is not well resolved. Although it occurs at depths of 5–10 km in most inversion models, some models show it extending deeper, and connecting with C0. Nevertheless, the spatial correlation of C2 with a significant fault and Au deposit suggests it could represent a fluid pathway.

The geological cause of proposed fluid-pathway conductors C1–C3 is interpreted to be iron sulfides and/or graphite produced by hydrothermal interaction of mineralizing fluids with surrounding rocks (e.g., Heinson et al., 2018; Hill et al., 2021; Comeau et al., 2022; Kirkby et al., 2022). Such minerals are orders of magnitude more conductive than minerals making up most of the crust and can produce strong conductivity anomalies even when present in only trace quantities if interconnected (e.g., Selway, 2014; Hill et al., 2021). Enhanced conductivity of C0, interpreted as the fluid source region, is also attributed to interconnected graphite and/or sulfides (e.g., Heinson et al., 2021; Hill et al., 2021; Comeau et al., 2022).

Kirkby et al. (2022) showed that conductors associated with mineral systems may be preserved for hundreds of millions of years, although they may be overprinted by late orogenic processes. Subduction-related conductors can also be preserved over long time scales (e.g., Ye et al., 2019). The middle- to lower-crustal conductors C0 and C1 are considered to be broadly coeval with the formation of the suture between the North Caribou and Winnipeg River terranes. Their interpretation as the source region for CO_2 - and Au-rich fluids and as fluid pathway conductors that produced the main-phase Red Lake greenstone belt mineralization requires them to have formed prior to 2.712 Ga. Much of later large-scale tectonic deformation involved reactivation of existing

structures (Sanborn-Barrie et al., 2004; Hrabi and Cruden, 2006). Thus, interconnected sulfide or graphite may have remained in shear zones during reactivation or even become more efficiently connected, preserving the signature of earlier fluid transport. The incomplete connection of the C2 and C3 conductors to the deposits and the relatively resistive crust beneath the Red Lake mine trend (<5 km) suggests the possibility of localized late overprinting of the fluid pathways affected by the intrusion of late- to post-orogenic granites (Sanborn-Barrie et al., 2001), thermal processes during the peak metamorphism associated with the intrusions, and/or development of extensional tectonic structures.

Tectonomagmatic processes in the Uchi terrane during the Red Lake greenstone belt Au mineralization were related to convergence between the Winnipeg River terrane and the Uchi–North Caribou crust, cessation of subduction, and delamination or slab break-off events (Corfu et al., 1995; Hrabi and Cruden, 2006). Formation of a 50-km-long north-south conductor at 20–25 km depth beneath the Red Lake greenstone belt and English River terrane would have required relatively widespread heat in order to have produced the temperatures required for development of flake graphite (Rosing-Schow et al., 2017) and/or resulted in the granulite facies metamorphism needed to produce the CO_2 - and Au-rich fluids (Chi et al., 2009). This may have resulted because of slab break-off or delamination of the subducted Winnipeg River terrane. Other processes that could have potentially produced significant crustal heating include southward migration of subduction and the interaction of subduction zone–derived melts with the overlying crust (Corfu and Stone, 1998).

There are several further aspects of the interpretation requiring explanation. Calvert et al. (2004) suggested that extensional tectonics associated with orogenic collapse at ca. 2.7 Ga may have been responsible for both crustal heating and the late-stage Au mineralization. Studies elsewhere, including MT investigations, have defined mineral systems in which Au-rich fluids are derived from mantle sources (e.g., Comeau et al., 2022). The Red Lake greenstone belt MT inversions do not preclude a moderately conductive zone in the mantle, so the data cannot exclude a mantle contribution. However, the large C0 conductor at mid- to lower-crustal depth is a more likely source for the majority of the fluids. Finally, it is possible the middle to lower crust beneath the Red Lake greenstone belt was previously enriched in Au-rich sulfides by mantle-derived fluids creating the source for the mineralization (e.g., Chi et al., 2009; Fu and Touret, 2014; Holwell et al., 2022). It is not possible to exclude such possibilities, but observation of a large subduction-related conductor (C1) and the capability of the devolatilization process of supracrustal rocks to provide the necessary

Au, S, and fluids for the mineral system (e.g., Pitcairn et al., 2015, Gaboury, 2019; Groves et al., 2020) provide strong support for the role of subducted supracrustal rocks.

ACKNOWLEDGMENTS

We thank Benoît Dubé, Rasmus Haugaard, Kate Selway, Andrew Calvert, and an anonymous reviewer for their valuable comments. This is Metal Earth publication MERC-ME-2022-22.

REFERENCES CITED

- Calvert, A.J., Cruden, A.R., and Hynes, A., 2004, Seismic evidence for preservation of the Archean Uchi granite-greenstone belt by crustal-scale extension: *Tectonophysics*, v. 388, p. 135–143, <https://doi.org/10.1016/j.tecto.2004.07.043>.
- Chi, G.X., Dubé, B., Williamson, K., and Williams-Jones, A.E., 2006, Formation of the Campbell–Red Lake gold deposit by H₂O-poor, CO₂-dominated fluids: *Mineralium Deposita*, v. 40, p. 726–741, <https://doi.org/10.1007/s00126-005-0029-3>.
- Chi, G.X., Liu, Y.X., and Dubé, B., 2009, Relationship between CO₂-dominated fluids, hydrothermal alterations and gold mineralization in the Red Lake greenstone belt, Canada: *Applied Geochemistry*, v. 24, p. 504–516, <https://doi.org/10.1016/j.apgeochem.2008.12.005>.
- Chi, G.X., Xu, D.R., Xue, C.J., Li, Z.H., Ledru, P., Deng, T., Wang, Y.M., and Song, H., 2022, Hydrodynamic links between shallow and deep mineralization systems and implications for deep mineral exploration: *Acta Geologica Sinica (English Edition)*, v. 96, p. 1–25, <https://doi.org/10.1111/1755-6724.14903>.
- Comeau, M.J., Becken, M. and Kuvshinov, A.V., 2022, Imaging the whole-lithosphere architecture of a mineral system—Geophysical signatures of the sources and pathways of ore-forming fluids: *Geochemistry, Geophysics, Geosystems*, v. 23, e2022GC010379, <https://doi.org/10.1029/2022GC010379>.
- Corfu, F., and Stone, D., 1998, Age structure and orogenic significance of the Berens River composite batholiths, western Superior Province: *Canadian Journal of Earth Sciences*, v. 35, p. 1089–1109, <https://doi.org/10.1139/e98-056>.
- Corfu, F., Stott, G.M., and Breaks, F.W., 1995, U-Pb geochronology and evolution of the English River Subprovince, an Archean low P–high T metasedimentary belt in the Superior Province: *Tectonics*, v. 14, p. 1220–1233, <https://doi.org/10.1029/95TC01452>.
- Dubé, B., Williamson, K., McNicoll, V., Malo, M., Skulski, T., Twomey, T., and Sanborn-Barrie, M., 2004, Timing of gold mineralization at Red Lake, northwestern Ontario, Canada: New constraints from U-Pb geochronology at the Goldcorp high-grade zone, Red Lake mine, and the Madsen mine: *Economic Geology*, v. 99, p. 1611–1641, <https://doi.org/10.2113/gsecongeo.99.8.1611>.
- Fu, B., and Touret, J.L.R., 2014, From granulite fluids to quartz-carbonate megashear zones: The gold rush: *Geoscience Frontiers*, v. 5, p. 747–758, <https://doi.org/10.1016/j.gsf.2014.03.013>.
- Gaboury, D., 2019, Parameters for the formation of orogenic gold deposits: *Transactions of the Institution of Mining and Metallurgy: Section B, Applied Earth Science*, v. 128, p. 124–133, <https://doi.org/10.1080/25726838.2019.1583310>.
- Gallagher, S., Camacho, A., Fayek, M., Epp, M., Spell, T.L., and Armstrong, R., 2018, Geology, geochemistry, and geochronology of the East Bay gold trend, Red Lake, Ontario, Canada: *Mineralium Deposita*, v. 53, p. 127–141, <https://doi.org/10.1007/s00126-017-0730-z>.
- Goldfarb, R.J., and Groves, D.L., 2015, Orogenic gold: Common or evolving fluid and metal sources through time: *Lithos*, v. 233, p. 2–26, <https://doi.org/10.1016/j.lithos.2015.07.011>.
- Groves, D.L., Santosh, M., and Zhang, L., 2020, A scale-integrated exploration model for orogenic gold deposits based on a mineral system approach: *Geoscience Frontiers*, v. 11, p. 719–738, <https://doi.org/10.1016/j.gsf.2019.12.007>.
- Heinson, G., Didana, Y., Soeffky, P., Thiel, S., and Wise, T., 2018, The crustal geophysical signature of a world-class magmatic mineral system: *Scientific Reports*, v. 8, 10608, <https://doi.org/10.1038/s41598-018-29016-2>.
- Heinson, G., Duan, J.M., Kirkby, A., Robertson, K., Thiel, S., Aivazpourpogou, S., and Soyer, W., 2021, Lower crustal resistivity signature of an orogenic gold system: *Scientific Reports*, v. 11, 15807, <https://doi.org/10.1038/s41598-021-94531-8>.
- Hill, G.J., Roots, E.A., Frieman, B.M., Haugaard, R., Craven, J.A., Smith, R.S., Snyder, D.B., Zhou, X., and Sherlock, R., 2021, On Archean craton growth and stabilisation: Insights from lithospheric resistivity structure of the Superior Province: *Earth and Planetary Science Letters*, v. 562, 116853, <https://doi.org/10.1016/j.epsl.2021.116853>.
- Holwell, D.A., Fiorentini, M.L., Knott, T.R., McDonald, I., Blanks, D.E., McCuaig, T.C., and Gorczyk, W., 2022, Mobilisation of deep crustal sulfide melts as a first order control on upper lithospheric metallogeny: *Nature Communications*, v. 13, 573, <https://doi.org/10.1038/s41467-022-28275-y>.
- Hrabi, B., and Cruden, A.R., 2006, Structure of the Archean English River subprovince: Implications for the tectonic evolution of the western Superior Province, Canada: *Canadian Journal of Earth Sciences*, v. 43, p. 947–966, <https://doi.org/10.1139/e06-023>.
- Kirkby, A., Czarnota, K., Huston, D.L., Champion, D.C., Doublier, M.P., Bedrosian, P.A., Duan, J.M., and Heinson, G., 2022, Lithospheric conductors reveal source regions of convergent margin mineral systems: *Scientific Reports*, v. 12, 8190, <https://doi.org/10.1038/s41598-022-11921-2>.
- Lewis, S.O., Ravnaas, C., Dorado-Troughton, M., Ferguson, S.A., Pettigrew, T.K., Dorland, G., and Patterson, C., 2021, Report of Activities, 2020: Resident Geologist Program—Red Lake Regional Resident Geologist Report: Red Lake and Kenora Districts: Ontario Geological Survey Open File Report 6371, 95 p.
- Percival, J.A., 2007, Geology and metallogeny of the Superior Province, Canada, in Goodfellow, W.D., ed., *Mineral Deposits of Canada: A Synthesis of Major Deposit-Types, District Metallogeny, the Evolution of Geological Provinces, and Exploration Methods*: Geological Association of Canada, Mineral Deposits Division, Special Publication 5, p. 903–928.
- Percival, J.A., McNicoll, V., and Bailes, A.H., 2006a, Strike-slip juxtaposition of ca. 2.72 Ga juvenile arc and >2.98 Ga continent margin sequences and its implications for Archean terrane accretion, western Superior Province, Canada: *Canadian Journal of Earth Sciences*, v. 43, p. 895–927, <https://doi.org/10.1139/e06-039>.
- Percival, J.A., Sanborn-Barrie, M., Skulski, T., Stott, G.M., Helmstaedt, H., and White, D.J., 2006b, Tectonic evolution of the western Superior Province from NATMAP and Lithoprobe studies: *Canadian Journal of Earth Sciences*, v. 43, p. 1085–1117, <https://doi.org/10.1139/e06-043>.
- Pitcairn, I.K., Craw, D., and Teagle, D.A.H., 2015, Metabasalts as sources of metals in orogenic gold deposits: *Mineralium Deposita*, v. 50, p. 373–390, <https://doi.org/10.1007/s00126-014-0547-y>.
- Rosing-Schow, N., Bagas, L., Kolb, J., Balić-Zunić, T., Korte, C., and Fiorentini, M.L., 2017, Hydrothermal flake graphite mineralisation in Paleoproterozoic rocks of south-east Greenland: *Mineralium Deposita*, v. 52, p. 769–789, <https://doi.org/10.1007/s00126-016-0701-9>.
- Sanborn-Barrie, M., and Skulski, T., 2006, Sedimentary and structural evidence for 2.7 Ga continental arc–oceanic-arc collision in the Savant-Sturgeon greenstone belt, western Superior Province, Canada: *Canadian Journal of Earth Sciences*, v. 43, p. 995–1030, <https://doi.org/10.1139/e06-060>.
- Sanborn-Barrie, M., Skulski, T., and Parker, J.R., 2001, Three hundred million years of tectonic history recorded by the Red Lake greenstone belt, Ontario: *Geological Survey of Canada Current Research 2001-C19*, <https://doi.org/10.4095/212109>.
- Sanborn-Barrie, M., Rogers, N., Skulski, T., Parker, J.R., and Devaney, J., 2004, Geology and tectonostratigraphic assemblages, east Uchi Subprovince, Red Lake and Birch-Uchi belts, Ontario: *Geological Survey of Canada Open File 4256 and Ontario Geological Survey Preliminary Map P3460*, Western Superior NATMAP Compilation Series, 1 sheet, scale 1:250,000, <https://doi.org/10.4095/215111>.
- Selway, K., 2014, On the causes of electrical conductivity anomalies in tectonically stable lithosphere: *Surveys in Geophysics*, v. 35, p. 219–257, <https://doi.org/10.1007/s10712-013-9235-1>.
- Vadoodi, R., Rasmussen, T.M., Smimov, M., and Bauer, T., 2021, Towards an understanding of mineral systems—Contributions from magnetotelluric data from the Fennoscandian Shield in northern Sweden: *Tectonophysics*, v. 808, 228816, <https://doi.org/10.1016/j.tecto.2021.228816>.
- van der Velden, A.J., 2007, Seismic reflection profiling of Neoproterozoic cratons [Ph.D. thesis]: Calgary, University of Calgary, 195 p., <https://doi.org/10.11575/PRISM/871>.
- Wannamaker, P.E., Caldwell, T.G., Jiracek, G.R., Maris, V., Hill, G.J., Ogawa, Y., Bibby, H.M., Bennie, S.L., and Heise, W., 2009, Fluid and deformation regime of an advancing subduction system at Marlborough, New Zealand: *Nature*, v. 460, p. 733–736, <https://doi.org/10.1038/nature08204>.
- White, D.J., Musacchio, G., Helmstaedt, H.H., Harrap, R.M., Thurston, P.C., van der Velden, A., and Hall, K., 2003, Images of a lower-crustal oceanic slab: Direct evidence for tectonic accretion in the Archean western Superior province: *Geology*, v. 31, p. 997–1000, <https://doi.org/10.1130/G20014.1>.
- Ye, G.F., Unsworth, M., Wei, W.B., Jin, S., and Liu, Z.L., 2019, The lithospheric structure of the Solonker Suture Zone and adjacent areas: Crustal anisotropy revealed by a high-resolution magnetotelluric study: *Journal of Geophysical Research: Solid Earth*, v. 124, p. 1142–1163, <https://doi.org/10.1029/2018JB015719>.
- Zeng, F.F., and Calvert, A.J., 2006, Imaging the upper part of the Red Lake greenstone belt, northwestern Ontario, with 3-D traveltimes tomography: *Canadian Journal of Earth Sciences*, v. 43, p. 849–863, <https://doi.org/10.1139/e06-027>.

Printed in USA